# Leveraging Fluorescent Emission to Unitary Yield: Dimerization of Polycyclic Aromatic Hydrocarbons

Tanja Miletić,[a] Nicolas Biot,[a] Nicola Demitri,[b] Giuseppe Brancato,[c] Benson M. Kariuki,[a] and Davide Bonifazi*[a]

[a] School of Chemistry, Cardiff University, Park Place, UK-CF10 3AT, Cardiff, e-mail: bonifazid@cardiff.ac.uk [b] Elettra-Sincrotrone Trieste, S.S. 14 Km 163.5 in Area Science Park, IT-34149 Basovizza-Trieste, Italy
[c] Scuola Normale Superiore, piazza dei Cavalieri 7, IT-56126 Pisa, Italy

Dedicated to Prof. *François Diederich* as a contribution to his farewell celebration and in recognition for his outstanding scientific achievements and mentorship.

We report on the synthesis and characterization of novel substituted 1,1'-biperylene-2,2'-diols in which the dihedral angle between the two polycyclic aromatic hydrocarbon (PAH) units is tailored from *ca.* 60° to *ca.* 90° in the solid state by introduction of cyclo-etheric straps or sterically hindered groups such as the triisopropylsilyl (TIPS) group. Depending on the type of substitution, we lock the dihedral angle between the perylenyl moieties enabling fine-tuning of the molecular optoelectronic properties, with the molecules displaying the smallest angles acting as exceptionally strong emitters with unitary quantum yields.

**Keywords:** dihedral angle, dipolycyclic aromatic hydrocarbons, chromophores, emitters, perylene.

## Introduction

Rational control of the dihedral angle between the *π*-conjugated fragments of molecular entities is one of the approaches used by organic chemists to finely tune the optoelectronic properties of polycyclic aromatic hydrocarbons.[1–7] Key examples include synthetic bacteriochlorins,[8] *meso meso* linked porphyrins,[2] extended naphthofurans,[4][9] and binaphthyl-derived polymers.[3][10] Among the different scaffolds, biaryls and its derivatives have certainly attracted the widest interest, as they can be used as ligands for asymmetric catalysis,[11–14] key structural elements in pharmacologically active substances,[15–17] agrochemicals,[17][18] supramolecular architectures,[19–26] mechanophores-based sensors,[27][28] and light-harvesting complexes,[29][30] to mention a few. In this context, chiral 1,1'-bi-2-naphthols (BINOLs) revealed to be a versatile building block for the construction of functional luminescent materials for fluorescent sensors,[31–37] metal organic frameworks (MOFs),[22][38] chiral polymers,[10][31][39] and molecular machines,[40–43] among others.

Very recently, we reported on the synthesis and characterization of a highly emissive *π*-extended 1,1'-biperylene-2,2'-diol ((±)-**2**$^{\mathbf{2H}}$)[7] featuring good solubility in organic solvents, blue-centered UV-Vis absorption and high fluorescence quantum yields ($\Phi$ ~ 0.9) when compared to that of its perylenyl precursor ($\Phi$ ~ 0.5).[7] When looking at the chemical structure of (±)-**2**$^{\mathbf{2H}}$, one can hardly fail to see that the free hydroxy groups of the biperylenediol moieties can be functionalized either with bridging units or bulky groups to gain control on the torsion angle (*Figures 1* and *2*) between the two perylenyl fragments of (±)-**2**$^{\mathbf{2H}}$.[44] It is in the light of this observation that we report on the synthesis, X-ray analysis, and photophysical properties of a series of 1,1'-biperylene-2,2'-diol derivatives, in which the torsion angle between the two perylenyl units is modulated by introducing either bridging cycloethers or sterically hindered TIPS substituents (*Figure 2*). As expected, the molecules featuring the

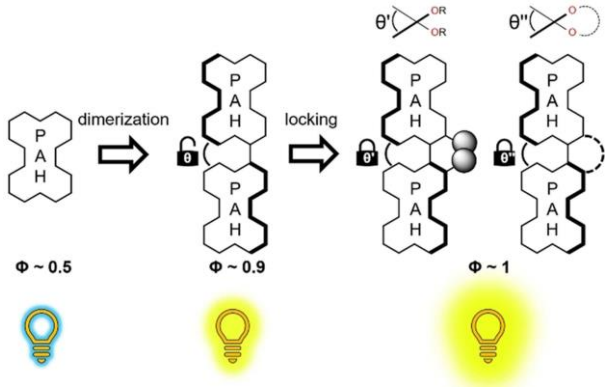


**Figure 1.** Schematic representation of the dimerization and locking of PAHs into highly fluorescent dimeric molecules. *θ*' = dihedral angle of open dimer and *θ*'' = dihedral angle of closed dimer. Quantum yield values of 0.5 and 0.9 for perylene and biperylene derivatives are taken from the literature.[7]

smallest angles displayed the strongest emissive properties.

## Results and Discussion

The synthetic conditions adopted for the preparation of 2,2'-functionalized biperylenediol derivatives **2$^{Acy}$** and **3$^{Cyc}$** are gathered in *Table 1*. Starting biperylene-diol (**±**)-**2$^{2H}$** and references (**±**)-**2$^{2Me}$** and (**±**)-**1$^{Fur}$** were prepared following a previously reported protocol (*Scheme S1*).[7]

Treatment of biperylenediol (**±**)-**2$^{2H}$** with TIPSCl in the presence of imidazole and DMAP in DMF[45] led to the formation of mono-TIPS substituted (**±**)-**2$^{HTips}$** and disubstituted derivative (**±**)-**2$^{2Tips}$** in 46% and 18% yield, respectively. Capitalizing on a double *Williamson* etherification reaction,[44][46] compound (**±**)-**2$^{2H}$** was reacted with the relevant benzyl- or alkyl halide in the presence of $K_2CO_3$ to form compounds (**±**)-**3$^{a}$**, (**±**)-**3$^{b}$**, and (**±**)-**3$^{d}$** in 97, 24, and 88% yield, respectively. In a like manner, compound (**±**)-**2$^{2H}$** underwent a tetra alkylation reaction[47] when treated very slowly with 1,2,4,5-tetrakis(bromomethyl)benzene in the presence of $K_2CO_3$ in anhydrous DMF at 80 °C yielding molecule **3$^{c}$** (*Table 1*, *Scheme S2*). Purification of the crude material through silica gel chromatography gave two distinct fractions that have been assigned to *meso*-(*R*,*S*)-**3$^{c}$** and racemic mixture of (*R*,*R*)-**3$^{c}$** and (*S*,*S*)-**3$^{c}$** ((**±**)-**3$^{c}$**). The molecular masses of both *meso* and racemic **3$^{c}$** were identified by HR-MALDI through the detection of the peaks at *m/z* 1867.1141 and 1867.1173, respectively ($M^+$, $C_{138}H_{146}O_4^+$; calc. 1867.1216). Solution $^1$H-NMR analysis of both samples showed highly symmetric spectra (*Figures 3,a* and *3,b*), with the biperylenyl moieties being chemically equiv-alent and the appearance of the typical *doublet* pattern of the diastereotopic methylene protons (see also below). Whereas molecule (**±**)-**3$^{c}$** is highly soluble, *meso*-**3$^{c}$** proved to be poorly soluble in most of the common organic solvents, which limited its spectro-scopic characterization. Only X-ray analysis allowed decisive discrimination between the two diaster-eoisomers giving unambiguous confirmation of their

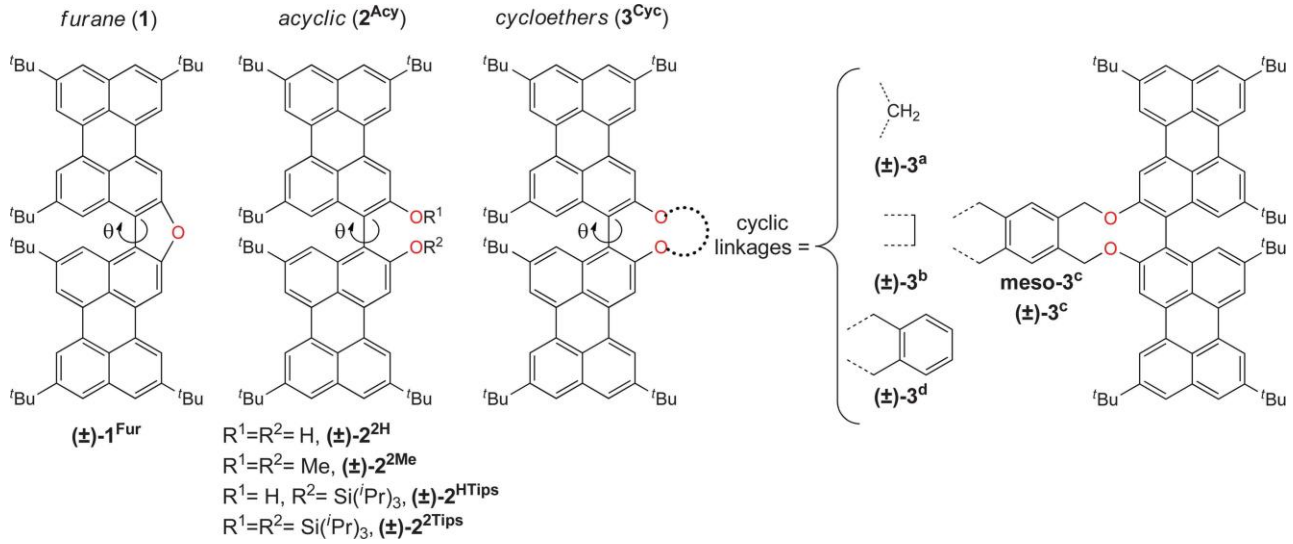


**Figure 2.** Chemical structure of 2,2'-functionalized biperylenediol derivatives investigated in this work.

**Table 1.** Synthetic protocol adopted for the preparation of acyclic **2**$^{HTips}$ and **2**$^{2Tips}$, and cyclic **3**$^{Cyc}$.

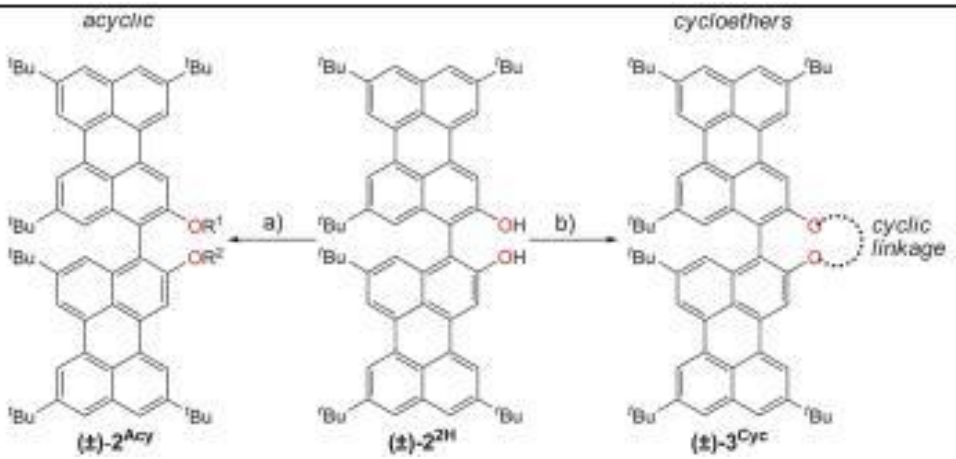


| Compound | O-substituents | Experimental conditions (a or b) | Yield [%] |
|---|---|---|---|
| (±)-**2**$^{HTips}$ | 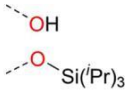 | a) imidazole, DMAP, TIPSCl, dry DMF, r.t., 24 h | 46 |
| (±)-**2**$^{2Tips}$ | 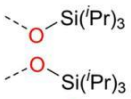 | a) imidazole, DMAP, TIPSCl, dry DMF, r.t., 24 h | 18 |
| (±)-**3**$^{a}$ |  | b) $CH_2Br_2$, $K_2CO_3$, NaI, dry acetone, reflux, 48 h | 97 |
| (±)-**3**$^{b}$ |  | b) $(CH_2)_2Br_2$, $K_2CO_3$, dry DMF, 80 °C, 48 h | 24 |
| **3**$^{c}$ | 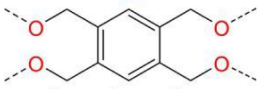 | b) 1,2,4,5-tetrakis (bromomethyl)benzene, $K_2CO_3$, dry DMF, 80 °C, 18 h | 62[a] |
| (±)-**3**$^{d}$ | 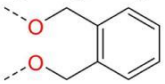 | b) *α*,*α*'-dibromo-*o*-xylene, $K_2CO_3$, dry DMF, 80 °C, 48 h | 88 |

[a]Total yield corresponding to *meso*-**3**$^{c}$ in 35% and (±)-**3**$^{c}$ in 27 % yield.

chemical and stereochemical identities (*Figure 6* below and *Section S6*).

Particular attention was paid to the two-folded tetrakis(methylenyl)benzene derivative (±)-**3**$^{c}$, which converts between two possible conformers: unfolded (U) and folded (F) (*Figure 4,b*). Dynamic properties of the conformation of (±)-**3**$^{c}$ were investigated through variable temperature (VT) $^1$H-NMR experiments in ($D_6$) acetone using a temperature range between 45 °C and 70 °C (*Figure 4,a*). $^1$H-NMR spectrum at r.t. shows the peaks of the aromatic H-atoms located between 7.1 and 8.6 ppm and two *doublet*s between 5.4 and 5.6 ppm that can be assigned to the diastereotopic methylene protons of the tetrakis(methylenyl) linkages (*Figure 3,b*). When the $^1$H-NMR spectrum of (±)-**3**$^{c}$ was recorded at 45 °C, no appreciable changes were detected except an improvement of the resolution without significant shifts of the methylene signals. However, upon decrease of the temperature from 45 °C to 70 °C, the two *doublet*s of the methylene protons undergo coalescence at 10 °C before splitting into four distinct doublets at 5.92, 5.64, 5.52, and 5.08 ppm at lower temperatures. The observed temperature-induced coalescence of the methylene proton resonances of (±)-**3**$^{c}$ suggests the presence of a dynamic equilibrium between the unfolded and folded conformers, with the dioxecine rings undergoing flipping motions.[43][47] The free-energy activation $G^{\ddagger}_{246}$ for the flipping could be estimated to be *ca.* 11.5 kcal mol$^{-1}$ using *Eyring*'s equation[47] (*Section S5*). All these observations suggested that the U and F conformers are in the slow exchange regime at low temperature and in fast exchange at high temperature.

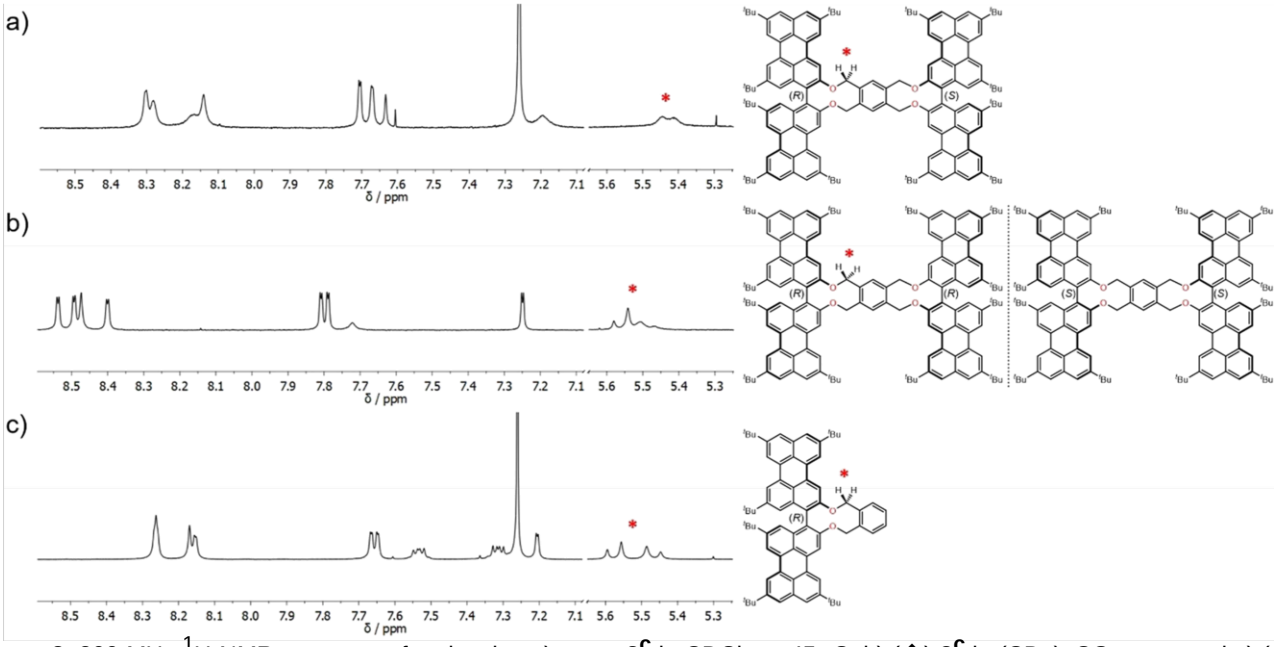


**Figure 3.** 300 MHz $^{1}$H-NMR spectrum of molecules a) *meso*-**3$^{c}$** in $CDCl_3$ at 45 °C, b) (±)-**3$^{c}$** in $(CD_3)_2CO$ at r.t., and c) (±)-**3$^{d}$** in $CDCl_3$ at r.t.

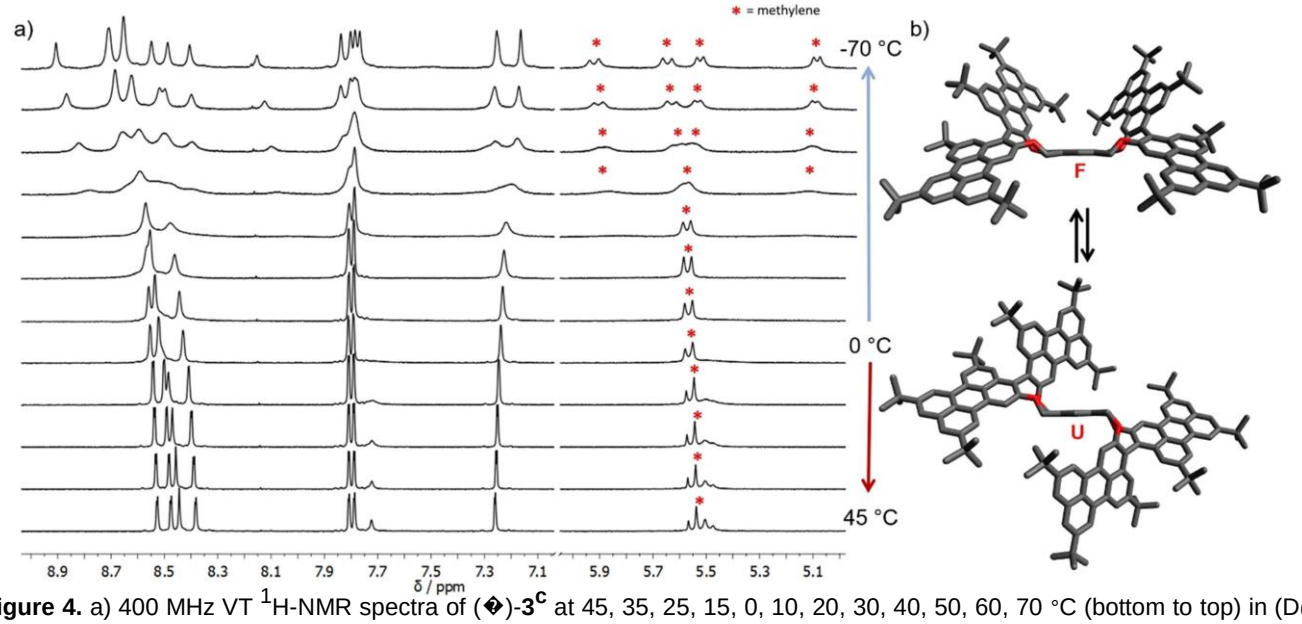


**Figure 4.** a) 400 MHz VT $^{1}$H-NMR spectra of (±)-**3$^{c}$** at 45, 35, 25, 15, 0, 10, 20, 30, 40, 50, 60, 70 °C (bottom to top) in $(D_6)$ acetone, and b) schematic representation of the conformational inversion process between the folded (F) and unfolded (U) conformers (hydrogens are omitted for clarity).

Crystals suitable for X-ray analysis were obtained for molecules (±)-**3$^{b}$**, *meso*-**3$^{c}$**, (±)-**3$^{c}$**, and (±)-**3$^{d}$** by vapor diffusion or slow evaporation of a dilute solution containing the relevant compound (see *Supporting Information* for detailed description, and *Figures 5* and *6*).

These crystal structures were compared with those of molecules (±)-**1$^{Fur}$** and (±)-**2$^{2H}$**, previously described by us.[7] *Figures 5,c* and *5,g* display the X-ray structure

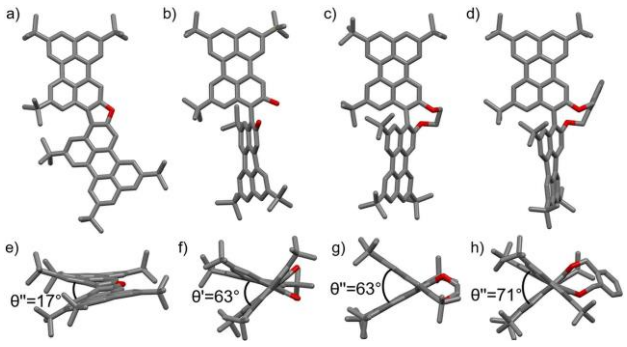


**Figure 5.** From the left: a–d) Top-view and e–h) side-view of the crystal structures of (±)-**1**$^{\mathbf{Fur}}$ (*P*2/*c*),[7] (±)-**2**$^{\mathbf{2H}}$ (*P*-1),[7] (±)-**3**$^{\mathbf{b}}$ (*Pn*), and (±)-**3**$^{\mathbf{d}}$ (*P*-1). All compounds crystallized as racemates. *θ*' = dihedral angle of open dimer and *θ*'' = dihedral angle of closed dimer.

of compound (±)-**3**$^{\mathbf{b}}$ bearing an ethane strap between the two hydroxy groups of the biperylenediol back-bone, which crystallized in space group *Pn* (see *Supporting Information* for crystallographic data and refinement details). The asymmetric unit contains two crystallographically independent molecules. The X-ray analyses of *meso*-**3**$^{\mathbf{c}}$ and (±)-**3**$^{\mathbf{c}}$ (*Figures S15*, *S16*, and *6*) show a butterfly-like structure for both compounds with their molecular symmetry being reflected in the solid-state arrangement. In both cases, the asymmetric unit contains half of the molecule, and the second half is generated through an inversion center for *meso*-**3**$^{\mathbf{c}}$ (space group *P*-1) and a two-fold rotation for (±)-**3**$^{\mathbf{c}}$ (space group *C*2/*c*). In the crystal packing of (±)-**3**$^{\mathbf{c}}$ both enantiomers (*R*,*R*) and (*S*,*S*) are equally present in an unfolded conformation[47] (*Figure 6*). For (±)-**3**$^{\mathbf{b}}$, *meso*-**3**$^{\mathbf{c}}$, and (±)-**3**$^{\mathbf{c}}$ only hydrophobic CH-*π* contacts are present, with the perylene moieties delimiting cavities filled either with $CH_2Br_2$ for (±)-**3**$^{\mathbf{b}}$, *meso*-**3**$^{\mathbf{c}}$, and acetone for (±)-**3**$^{\mathbf{c}}$. For molecule (±)-**3**$^{\mathbf{d}}$ (*Figures 5,d* and *5,h*), the crystal packing shows limited perylene π−*π* stacking between symmetry-related molecules. Also, in this case, the perylene motifs delimit cavities filled by solvent ($CH_2Cl_2$). In all investigated com-pounds, the rotation around the bond 1,1' is restricted by the alkoxy groups, where the ethane bridge in (±)-**3**$^{\mathbf{b}}$ defines an eight-membered ring whereas a ten-membered ring is present for the dibenzylene-bridged derivatives *meso*-**3**$^{\mathbf{c}}$, (±)-**3**$^{\mathbf{c}}$, and (±)-**3**$^{\mathbf{d}}$. As expected, the dimension of the ring directly influences the dihedral angle between the two perylene fragments. In fact, the smaller the ring formed is, the more constrained the perylene moieties to smaller angles (*Figures 5e– h* and *6*). Crystallographic data reported for reference compounds (±)-**1**$^{\mathbf{Fur}}$ and (±)-**2**$^{\mathbf{2H}}$ show a large decrease of the dihedral angle from 63° for (±)-**2**$^{\mathbf{2H}}$ to 17° for (±)-**1**$^{\mathbf{Fur}}$, where the dihedral angle between the aryl moieties is drastically reduced by planarity of the furanyl framework.[7] In order to further corroborate the locked angle of the biperylenediols, geometry optimization in gas phase for each derivative has been performed using Gaussian09[48] including the D01 revision at B3LYP/6-31 + G(d,p) level of theory. Data are gathered in *Table 2*. The results show a larger angle value for the molecules bearing bulkier substituents and larger cyclic linkages for **2**$^{\mathbf{Acy}}$ and **3**$^{\mathbf{Cyc}}$, respectively in accordance with experimental results. The only exception is (±)-**2**$^{\mathbf{2H}}$ that presents a smaller experimental dihedral angle of 62°, whereas the calculated value is 79°. This could be rationalized by a less hindered motion of the two perylene units along the 1,1' bond in the gas phase giving a larger value. On the other hand, *meso*-**3**$^{\mathbf{c}}$ shows an exper-

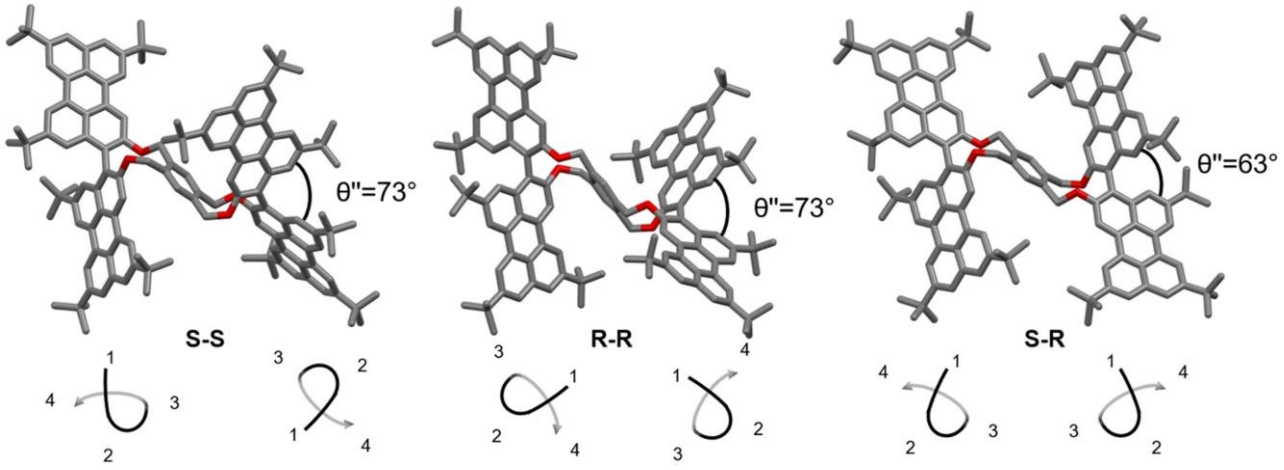


**Figure 6.** Crystal structures of **3**$^{\mathbf{c}}$. a) (*S*,*S*)-**3**$^{\mathbf{c}}$, b) (*R*,*R*)-**3**$^{\mathbf{c}}$ (*C*2/*c*), and c) *meso*-**3**$^{\mathbf{c}}$ (*P*-1). *θ*'' = dihedral angle of closed dimer.

**Table 2.** Angles between the two mean planes of each perylene units in the crystal ($\theta_{exp}$) and computed ($\theta_{cal}$) structures.

| **2**[Acy][a] | θ' | | θ'' | | **3**[Cyc][b] |
|---|---|---|---|---|---|
| | $\theta_{exp}$ | $\theta_{cal}$ [c] | $\theta_{cal}$ [c] | $\theta_{exp}$ | |
| (±)-**2**$^{2H}$ | 62 | 79 | 62 | –[d] | (±)-**3**$^{a}$ |
| (±)-**2**$^{2Me}$ | –[d] | 79 | 70 | 63 | (±)-**3**$^{b}$ |
| (±)-**2**$^{HTips}$ | –[d] | 81 | –[e] | 73 | (±)-**3**$^{c}$ |
| (±)-**2**$^{2Tips}$ | –[d] | 89 | –[e] | 63 | *meso*-**3**$^{c}$ |
| | | | 73 | 71 | (±)-**3**$^{d}$ |

[a] $\theta'$ = dihedral angle of open dimer and [b] $\theta''$ = dihedral angle of closed dimer. [c] Calculation performed at B3LYP/6-31 + G(d, p) level of theory using Gaussian09 including the D01 revision. [d] No single crystals suitable for X-ray diffraction could be grown. [e] No convergence has been reached for those molecules.

imental torsion angle of 63°, the smallest among the dioxecine derivatives (±)-**3**$^{c/d}$, which can be ascribed to the presence of entrapped crystalline solvent molecules ($CH_2Br_2$).

Steady-state UV/Vis absorption and emission spectroscopy has been used to study the effects of the dihedral angle on the optical properties of (±)-**2**$^{Acy}$ and (±)-**3**$^{Cyc}$ using (±)-**2**$^{2Me}$ and (±)-**1**$^{Fur}$ as references. Measurements in aerated toluene at r.t. are shown in *Figure 7*, and the main results are gathered in *Table 3*.

As a general trend, the absorption and emission spectra of (±)-**2**$^{Acy}$ and (±)-**3**$^{Cyc}$ show the characteristic features of biperylenediols,[7] with gradual bathochro-mic shift upon shrinking the dihedral angle between the two perylenyl fragments. Indeed, compound (±)-**3**$^{a}$ containing a dioxepin system ($\theta''$ = 62°) exhibits a maximum absorption peak centered at 484 nm, *ca.*

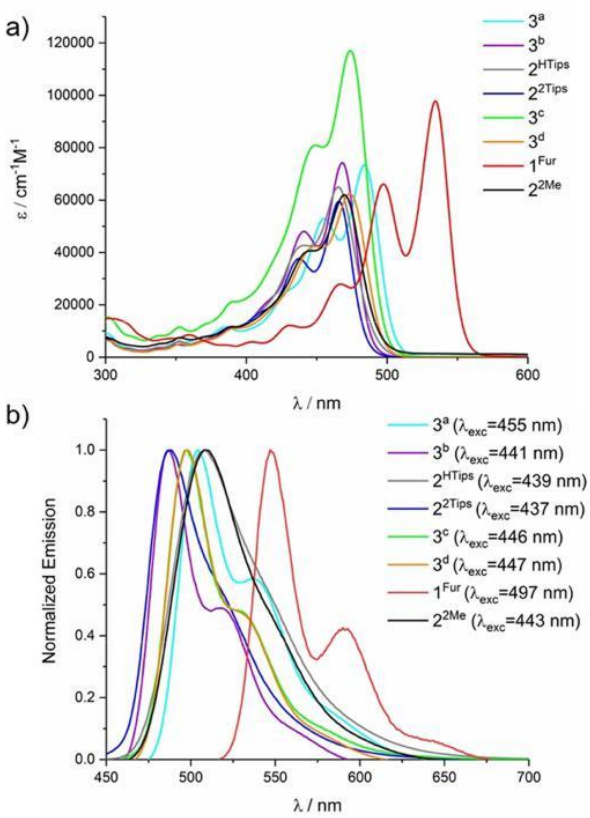


**Figure 7.** a) Absorption and b) emission spectra of compounds (±)-$1^{Fur}$, (±)-$2^{Acy}$, and (±)-$3^{Cyc}$ in air-equilibrated toluene at r.t.

20 nm red-shifted compared to (±)-**2**$^{2Tips}$ bearing bulky TIPS groups at the OH termini ($\theta'$ = 89°, $\lambda_{max}$ = 466 nm). However, little positional variation of the absorption maxima was observed for the acyclic molecules (±)-**2**$^{2Me}$, (±)-**2**$^{HTips}$, and (±)-**2**$^{2Tips}$ ($\lambda_{max}$ = 470, 465, and 466 nm, respectively). Reference (±)-**1**$^{Fur}$

**Table 3.** Optical properties of the 2,2'-functionalized biperylenediol derivatives.

| Molecule/$\theta$ [°] | $\lambda_{abs}$ [nm][a], $E$ [$M^{-1}$ $cm^{-1}$] | $\lambda_{em}$ [nm][b] | $\Phi$ | Stokes shift [nm] |
|---|---|---|---|---|
| (±)-**1**$^{Fur}$/16.7[c] | 534, 97400[d] | 547[d] | 0.8[d] | 13 (445 $cm^{-1}$) |
| (±)-**2**$^{2H}$/62[c] | 463, 65000[d] | 472[d] | 0.88[d] | 9 (411 $cm^{-1}$) |
| (±)-**2**$^{2Me}$/80[e] | 470, 59500 | 509 | 0.97 | 39 (1630 $cm^{-1}$) |
| (±)-**2**$^{HTips}$/81[e] | 465, 64900 | 508 | 0.95 | 43 (1820 $cm^{-1}$) |
| (±)-**2**$^{2Tips}$/89[e] | 466, 59000 | 487 | 0.97 | 21 (925 $cm^{-1}$) |
| (±)-**3**$^{a}$/63[e] | 484, 72600 | 504 | 0.92 | 20 (820 $cm^{-1}$) |
| (±)-**3**$^{b}$/69[e] | 468, 72500 | 487 | 1.0 | 19 (834 $cm^{-1}$) |
| (±)-**3**$^{c}$/73[c] | 474, 115800 | 497 | 1.0 | 23 (976 $cm^{-1}$) |
| (±)-**3**$^{d}$/71[c] | 474, 61400 | 498 | 1.0 | 24 (1017 $cm^{-1}$) |

[a] UV/Vis absorption maximum of the lowest-energy band in toluene at r.t. [b] Emission maximum in toluene at r.t. [c] Calculated from the crystal structure. [d] Data taken from reference.[7] [e] Optimized values using Gaussian09 including the D01 revision at B3LYP/6-31 + G(d,p) level of theory.

shows a maximum absorption band at 534 nm, which is strongly shifted toward the red compared to the other derivatives. As expected, the smaller the dihedral angle is, the larger the bathochromic shift is. Low dihedral angles favor a significant *π*-conjugation, over the entire molecule. All the investigated compounds present good molar absorptivity ($\varepsilon$ = 60 – 70 000 $M^{-1}$ $cm^{-1}$), with molecule (±)-**3$^{C}$** being the stron-gest absorber ($\varepsilon$ = 115800 $M^{-1}$ $cm^{-1}$). Obviously, the stronger absorption intensity is attributed to the presence of a second biperylenediol unit. As expected, the emission spectra slightly varied as a function of the dihedral angle between two adjacent perylenes. Exceptionally, molecules (±)-**2$^{HTips}$**, **2$^{2Tips}$**, and (±)-**3$^{Cyc}$** exhibit emissions between 487 and 509 nm with unitary fluorescence quantum yields ($\Phi$ ~1). Moreover, all bridged compounds ((±)-**1$^{Fur}$**, (±)-**3$^{Cyc}$**) present relatively small *Stokes* shifts (13 –24 nm) when compared to non-bridged derivatives ((±)-**2$^{2Me}$**, (±)-**2$^{HTips}$**), further supporting the idea that these molecules are conformationally rigid with the exception of (±)-**2$^{2Tips}$**.

## Conclusions

A novel class of substituted 1,1'-biperylene-2,2'-diols bearing either cyclo-ethers or bulky substituents at the OH termini have been prepared exploiting a facile synthetic route and characterized by means of X-ray analysis, UV-Vis absorption, and emission spectroscopy as well as theoretical calculations. Locking the dihedral angle between the two perylenyl fragments lead to the fine-tuning of the molecular optoelectronic prop-erties resulting in highly emissive bi-PAHs with unitary quantum yields. Moreover, capitalizing on a facile tetra-alkylation reaction, we synthesized a two-folded tetrakis(methylenyl)benzene derivative (±)-**3c**, which converts between an unfolded (U) and folded (F) conformation. The dynamic equilibrium between the two conformers (U and F), with the dioxecine rings undergoing flipping motions has been confirmed by VT $^{1}$H-NMR experiments. We believe that this work is of significant importance in the discovery of novel highly emissive luminescent compounds for a vast range of applications. For instance, by accessing enantiopure biperylenol frameworks one could engi-neer polarized emitters that could be used for sensing chiral species or inducing supramolecular chirality at the soft matter level.

## Experimental Section

*General*

Instruments, materials, and general methods are detailed in the *Supporting Information.*

*Experimental*

**5,5',8,8',11,11'-Hexa-*tert*-butyl-2'-{[tri(propan-2-yl)silyl]oxy}[3,3'-biperylen]-2-ol** ((±)-**2$^{HTips}$**) and **[(5,5',8,8',11,11'-Hexa-*tert*-butyl[3,3'-biperylene]-2,2'-diyl)bis(oxy)]bis[tri(propan-2-yl)silane]** ((±)-**2$^{2Tips}$**). Compounds (±)-**2$^{HTips}$** and (±)-**2$^{2Tips}$** were afforded following a slightly modified synthetic protocol reported for binaphthol derivatives.[45] In a flame-dried two-neck round bottom flask, biperylenol (±)-**2$^{2H}$** (20.0 mg, 0.02 mmol), imidazole (3.5 mg, 0.05 mmol), and 4-(dimethylamino)pyridine (DMAP, 6.2 mg, 0.05 mmol) were dissolved in anhydrous DMF (1 mL). The mixture was degassed by freeze-pump-thaw procedure and triisopropylsilyl chloride (TIPSCl, 11 µL, 0.05 mmol) added to the solution. The mixture was thus stirred at r.t. for 24 h under $N_2$ atmosphere. Brine (10 mL) was added, and the aqueous phase extracted with $CH_2Cl_2$ (5 × 15 mL). The combined organic layers were additionally washed with $H_2O$ (2 × 20 mL) and dried over $Na_2SO_4$. The crude product was purified by preparative TLC ($SiO_2$, eluents: petroleum ether/toluene, 8:2) to afford mono-triisopropylsilyl derivative (±)-**2$^{HTips}$** (11.0 mg, 46%) as bright yellow solid and di-triisopropylsilyl derivative (±)-**2$^{2Tips}$** (5.0 mg, 18%) as yellow solid.

*Characterization of* (±)-**2$^{HTips}$**. M.p.: > 160 –163 °C. UV-Vis (toluene): 465 nm ($\varepsilon$ = 64900 $M^{-1}$ $cm^{-1}$). FT-IR (ATR): 2953, 2864, 1601, 1460, 1431, 1362, 1254, 1211, 1182, 1082, 922, 872, 814, 681, 637. $^{1}$H-NMR (300 MHz, $(CD_3)_2CO$): 8.52 (*d*, *J*(H,H) = 1.8, 1 H); 8.48 (*d*, *J*(H,H) = 1.7, 1 H); 8.45 (*d*, *J*(H,H) = 1.8, 1 H); 8.41 (*d*, *J*(H,H) = 1.7, 1 H); 8.33 (*d*, *J*(H,H) = 1.8, 1 H); 8.30 (*d*, *J*(H,H) = 1.8, 1 H); 8.17 (*s*, 1 H); 8.06 (*s*, 1 H); 7.84 (*d*, *J*(H,H) = 1.7, 1 H); 7.82 (*d*, *J*(H,H) = 1.6, 1 H); 7.80 (*d*, *J*(H,H) = 1.6, 1 H); 7.78 (*d*, *J* (H,H) = 1.7, 1 H); 7.72 (*s*, 1 H); 1.54 (*s*, 9 H); 1.53– 1.50 (*m*, 27 H); 1.21 (*s*, 10 H); 1.19 (*s*, 9 H); 1.00 (*d*, *J*(H,H) = 7.4, 9 H); 0.95 (*d*, *J*(H,H) = 7.4, 9 H); 0.91– 0.84 (*m*, 3 H). $^{13}$C-NMR (150 MHz, $(CD_3)_2CO$): 154.7; 154.5; 153.8; 150.2; 149.9; 149.8; 149.4; 137.2; 136.6; 136.1; 136.0; 133.2; 133.0; 131.9; 131.7; 131.6; 131.3; 124.2; 123.6; 122.4; 122.2; 121.0; 119.4; 119.1; 119.0; 118.6; 117.5; 117.4; 116.8; 114.2; 112.0; 111.9; 35.6; 35.6; 35.5; 35.5; 31.6; 31.4; 30.3; 29.8; 18.3; 18.3; 13.7 (some peaks are

missing due to overlap). HR-ESI-MS: 1027.6788 ([*M* + H]$^+$, $C_{73}H_{91}O_2Si^+$; calc. 1027.6788).

Characterization of (**±**)-**2$^{2Tips}$**. M.p.: 189 –192 °C. UV-Vis (toluene): 466 nm ($\varepsilon$ = 59 000 $M^{-1}$ $cm^{-1}$). FT-IR (ATR): 2951, 2924, 2864, 1601, 1508, 1462, 1431, 1393, 1368, 1348, 1337, 1254, 1178, 1082, 1040, 1013, 997, 959, 924, 860, 816, 789, 739, 681, 636. $^1$H-NMR (300 MHz, $(CD_3)_2CO$): 8.51 (*d*, *J*(H,H) = 1.7, 2 H); 8.37 (*d*, *J*(H,H) = 1.7, 2 H); 8.30 (*d*, *J*(H,H) = 1.7, 2 H); 8.07 (*s*, 1 H); 7.82 (*d*, *J*(H,H) = 1.5, 2 H); 7.80 (*d*, *J*(H,H) = 1.5, 2 H); 7.19 (*d*, *J*(H,H) = 1.7, 2 H); 1.52 (*s*, 18 H); 1.51 (*s*, 18 H); 1.18 (*s*, 18 H); 1.01 (*d*, *J*(H,H) = 7.4, 18 H); 0.94– 0.83 (*m*, 24 H). $^{13}$C-NMR (150 MHz, $(CD_3)_2CO$): 153.4; 150.1; 149.7; 149.6; 136.8; 136.1; 132.6; 131.8; 131.7; 131.2; 126.3;
124.8; 124.3; 124.0; 122.9; 122.6; 119.3; 118.4; 117.4; 114.1; 35.6; 35.5; 35.5; 31.6; 31.3; 29.8; 18.5; 18.4; 13.7 (some peaks are missing due to overlap). HR-ASAP-MS: 1183.8131 ([*M* + H]$^+$, $C_{82}H_{111}O_2Si_2^+$; calc. 1183.8123).

**2,5,13,16,19,22-Hexa-*tert*-butyl-9*H*-diperylo[2,3-*d*:3',2'-*f*][1,3]dioxepine** ((**±**)-**3$^a$**). To a stirred mixture of compound (**±**)-**2$^{2H}$** (30.0 mg, 34.0 µmol), NaI (cata-lytic amount), and $K_2CO_3$ (30.0 mg, 220.0 µmol) in acetone (2 mL) at 60 °C under Ar, $CH_2Br_2$ (10 µL, 136.0 µmol) was added, and the mixture refluxed for 48 h. After cooling to r.t., the solvent was removed *in vacuo* and the residue dissolved in $CH_2Cl_2$ (10 mL) and washed with $H_2O$ (3 ×15 mL) and brine (15 mL). The organic layer was dried over $Na_2SO_4$ and evaporated under reduced pressure. The crude mixture was purified by column chromatography ($SiO_2$, eluents: cyclohexane/toluene, 9.5:0.5) to afford compound (**±**)-**3$^a$** (29.0 mg, 97 %) as yellow solid. M.p.: > 300 °C. UV-Vis (toluene): 484 nm ($\varepsilon$ = 72 600 $M^{-1}$ $cm^{-1}$). FT-IR (ATR): 3061, 2953, 2905, 2868, 1599, 1477, 1462, 1437, 1393, 1362, 1339, 1327, 1256, 1207, 1177, 1142, 1105, 1084, 1024, 1011, 991, 955, 918, 897, 874, 824, 808, 799, 787, 756, 716, 635. $^1$H-NMR (500 MHz, $CD_2Cl_2$): 8.37 (*d*, *J*(H,H) = 1.1, 2 H); 8.35 (*d*, *J*(H,H) = 1.3, 2 H); 8.33 (*d*, *J*(H,H) = 1.1, 2 H); 8.20 (*s*, 2 H); 7.74 (*d*, *J* (H,H) = 1.3, 2 H); 7.73 (*d*, *J*(H,H) = 1.1, 2 H); 7.42 (*d*, *J*(H,H) = 1.1, 2 H); 5.82 (*s*, 2 H); 1.53 (*s*, 18 H); 1.52 (*s*, 18 H); 1.21 (*s*, 18 H). $^{13}$C-NMR (125 MHz, $CD_2Cl_2$): 152.8; 149.8; 149.8; 149.5; 135.4; 134.2; 134.1; 131.8; 131.0; 130.4; 126.3; 125.6;
124.7; 124.3; 122.9; 119.5; 119.0; 118.6; 114.4; 103.4; 35.5; 35.5; 35.4; 31.7; 31.6; 31.3 (some peaks are missing due to overlap). HR-MALDI-MS: 882.5356 ($M^+$, $C_{65}H_{70}O_2^+$; calc. 882.5376).

**2,5,14,17,20,23-Hexa-*tert*-butyl-9,10-dihydrodiperylo[2,3-*e*:3',2'-*g*][1,4]dioxocine** ((**±**)-**3$^b$**). To a stirred mixture of compound (**±**)-**2$^{2H}$** (40.0 mg, 46.0 µmol) and $K_2CO_3$ (14.0 mg, 102.2 µmol) in anhy-drous DMF (2.0 mL), $(CH_2)_2Br_2$ (7.0 µL, 55.2 µmol) was added dropwise, and the mixture degassed following freeze-pump-thaw protocol. The mixture was stirred at 80 °C for 48 h under Ar atmosphere and then cooled to r.t. The solvent was removed *in vacuo*, the residue dissolved in $CH_2Cl_2$ (10 mL), and then washed with $H_2O$ (3 ×15 mL) and brine (15 mL). The organic layer was dried over $Na_2SO_4$ and evaporated under reduced pressure. The crude mixture was purified by column chromatography ($SiO_2$, eluents: cyclohexane/toluene, 8:2) to afford compound (**±**)-**3$^b$** (10.0 mg, 24%) as yellow solid. M.p.: > 300 °C. UV-Vis (toluene): 468 nm ($\varepsilon$ = 72600 $M^{-1}$ $cm^{-1}$). FT-IR (ATR): 2951, 2907, 2866, 2905, 1585, 1477, 1460, 1431, 1393, 1362, 1339, 1325, 1256, 1223, 1207, 1179, 1146, 1103, 1082, 982, 957, 928, 897, 876, 824, 808, 754, 721, 640, 619. $^1$H-NMR (500 MHz, $CD_2Cl_2$): 8.35 (*d*, *J*(H,H) = 1.5, 2 H); 8.34 (*d*, *J* (H,H) = 1.0, 2 H); 8.28 (*d*, *J*(H,H) = 1.0, 2 H); 8.18 (*s*, 2 H); 7.74 (*d*, *J*(H,H) = 1.5, 2 H); 7.72 (*d*, *J*(H,H) = 1.0, 2 H); 7.20 (*d*, *J*(H,H) = 1.0, 2 H); 4.56 (*d*, *J* (H,H) = 9.0, 2 H); 4.33 (*d*, *J*(H,H) = 9.0, 2 H); 1.53 (*s*, 18 H); 1.52 (*s*, 18 H); 1.14 (*s*, 18 H). $^{13}$C-NMR (125 MHz, $CD_2Cl_2$): 158.1; 149.7; 149.7; 149.6; 135.4; 135.0; 134.4; 131.5; 131.1; 130.4; 125.7;
125.4; 124.6; 124.6; 124.1; 123.6; 119.3; 118.8; 118.1; 116.0; 74.1; 35.5; 35.4; 35.3; 31.6; 31.3 (some peaks are missing due to overlap). HR-MALDI-MS: 896.5521 ($M^+$, $C_{66}H_{72}O_2^+$; calc. 896.5532). Despite several crystallization trials, only poorly diffracting crystals could be obtained by slow diffusion from a $CH_2Br_2$/MeOH solution and were characterized by synchrotron X-ray diffraction (see *Supporting Information*, *Section S6*).

**2,5,15,18,21,24,27,30,40,43,46,49-Dodeca-*tert*-butyl-11,36-dihydro-9*H*,34*H*-benzo[1,2-*c*:4,5-*c*']tetraperylo[2,3-*g*:2,3-*g*':3,2-*i*:3,2-*i*']bis[1,6]dioxecine** ((**±**)-**3$^c$** and *meso*-**3$^c$**). To a degassed solution of compound (**±**)-**2$^{2H}$** (40.0 mg, 45.0 µmol) and $K_2CO_3$ (22.0 mg, 160.0 µmol) in anhydrous DMF (1 mL) under $N_2$ at 80 °C, a solution of 1,2,4,5-tetrakis(bromomethyl) benzene (9.0 mg, 20.0 µmol) in anhydrous DMF (2 mL) was added dropwise over 2 h using a syringe pump. The mixture was stirred for additional 16 h at 80 °C under $N_2$ atmosphere. After cooling to r.t., the mixture was filtered over *Celite*®, washed with $CH_2Cl_2$, and the solvents were removed under reduced pressure. The crude mixture was purified by preparative TLC ($SiO_2$, eluents: petroleum ether/$CH_2Cl_2$, 6 :4) to afford two distinguishable diastereoisomers, (**±**)-**3$^c$** (10.0 mg) as yellow solid, and *meso*-**3$^c$** (13.0 mg) as dark yellow solid evaporated from MeOH (total yield = 62%).

Characterization of (±)-**3$^{c}$**. M.p.: > 300 °C. UV-Vis (toluene): 474 nm ($\varepsilon$ = 115 800 $M^{-1}$ $cm^{-1}$). FT-IR (ATR): 2953, 2870, 1601, 1477, 1462, 1433, 1393, 1364, 1341, 1323, 1256, 1207, 1177, 1140, 1072, 1026, 966, 895, 872, 824, 787, 727, 636. $^{1}$H-NMR (300 MHz, $(CD_3)_2CO$): 8.54 (*d*, *J*(H,H) = 1.5, 4 H); 8.49 (*d*, *J*(H,H) = 1.5, 4 H); 8.47 (*s*, 4 H); 8.40 (*d*, *J*(H,H) = 1.5, 4 H); 7.81 (*d*, *J*(H,H) = 1.5, 4 H); 7.79 (*d*, *J*(H,H) = 1.5, 4 H); 7.72 (*s*, 2 H); 7.25 (*d*, *J* (H,H) = 1.5, 4 H); 5.56 (*d*, *J*(H,H) = 12.0, 4 H); 5.49 (*d*, *J* (H,H) = 12.0, 4 H); 1.62 (*s*, 36 H); 1.50 (*s*, 36 H); 1.18 (*s*, 36 H). $^{13}$C-NMR (150 MHz, $(CD_3)_2CO$): 150.0; 150.0; 149.8; 138.3; 136.0; 135.7; 132.0; 131.5; 131.0; 126.2; 124.7; 124.6; 122.7; 119.4; 119.3; 117.8; 35.7; 35.6; 35.5; 31.8; 31.6; 31.3; 30.3 (some peaks are missing due to overlap). HR-MALDI-MS: 1867.1173 ($M^{+}$, $C_{138}H_{146}O_4^{+}$; calc. 1867.1216). Crystal suitable for X-ray diffraction was obtained by slow evaporation of an acetone solution (see *Supporting Information*, *Section S6*).

Characterization of *meso*-**3$^{c}$**. M.p.: > 300 °C. FT-IR (ATR): 2953, 2918, 2868, 2851, 1599, 1585, 1475, 1462, 1431, 1393, 1364, 1341, 1323, 1256, 1209, 1157, 1138, 1074, 1028, 966, 893, 824, 793, 748, 727, 638. $^{1}$H-NMR (300 MHz, $CDCl_3$, 45 °C): 8.32 – 8.26 (*m*, 8 H); 8.20– 8.11 (*m*, 8 H); 7.71 (*d*, *J*(H,H) = 1.5, 4 H); 7.67 (*d*, *J*(H,H) = 1.3, 4 H); 7.63 (*s*, 2 H); 7.19 (*s*, 4 H); 5.43 (*d*, *J*(H,H) = 8.6, 8 H); 1.51 (*s*, 72 H); 1.14 (*s*, 36 H). The poor solubility of *meso*-**3$^{c}$** in most of the commonly used organic solvents limited its characterization by $^{13}$C-NMR spectroscopy. HR-MALDI-MS: 1867.1141 ($M^{+}$, $C_{138}H_{146}O_4^{+}$; calc. 1867.1216). Crystal suitable for X-ray diffraction was obtained by slow diffusion of MeOH in a $CH_2Br_2$ solution (see *Supporting Information*, *Section S6*).

**2,5,18,21,24,27-Hexa-*tert*-butyl-9,14-dihydrobenzo[*h*]diperylo[2,3-*b*:3',2'-*d*][1,6]dioxecine** ((±)-**3$^{d}$**). To a stirred mixture of compound (±)-**2$^{2H}$** (30.0 mg, 34.0 μmol) and $K_2CO_3$ (10.4 mg, 75.0 μmol) in anhydrous DMF (2 mL), 1,2-bis(bromomethyl) benzene (10.0 mg, 34.0 μmol) was added dropwise, and the mixture degassed following the freeze-pump-thaw protocol. The mixture was stirred at 80 °C for 48 h under Ar atmosphere. After cooling down to r.t., the mixture was poured into $H_2O$ (10 mL) and extracted with $CH_2Cl_2$ (3 × 15 mL). The organic layer was subsequently washed with $H_2O$ (2 × 20 mL) and brine (20 mL) and dried over $Na_2SO_4$. The solvent was removed *in vacuo*, and the crude mixture was purified by column chromatography ($SiO_2$, eluents: cyclohexane/toluene, 9: 1) to afford compound (±)-**3$^{d}$** (29.0 mg, 88%) as yellow solid. M.p.: > 300 °C. UV-Vis (toluene): 474 nm (e = 61500 $M^{-1}$ $cm^{-1}$). IR (KBr): 2951, 2905, 2876, 1599, 1587, 1474, 1460, 1431, 1393, 1364, 1341, 1323, 1256, 1232, 1211, 1177, 1157, 2905, 1103, 1086, 1070, 1026, 999, 970, 959, 937, 920, 895, 878, 868, 854, 847, 824, 793, 752, 735, 723, 671, 640, 625, 586, 565, 548, 511. $^{1}$H-NMR (500 MHz, $CD_2Cl_2$): 8.32 – 8.29 (*m*, 4 H); 8.21 (*s*, 4 H); 7.72 (*s*, 2 H); 7.70 (*s*, 2 H); 7.56 (*dd* appearing *t*, *J*(H,H) = 4.5, 2 H); 7.34 (*dd, J*(H,H) = 4.5, 3.5, 2 H); 7.21 (*s*, 2 H); 5.58 (*d*, *J*(H,H) = 11.5, 2 H); 5.46 (*d*, *J*(H,H) = 11.5, 2 H); 1.57 (*s*, 18 H); 1.51 (*s*, 18 H); 1.16 (*s*, 18 H). $^{13}$C-NMR (125 MHz, $CD_2Cl_2$): 149.6; 149.6; 149.6; 136.9; 135.4; 135.2; 132.7; 132.0; 131.5; 131.2; 130.7; 129.5; 125.8; 124.3; 124.3; 124.0; 122.5; 122.4; 118.8; 118.7; 117.5; 110.8; 72.7; 35.5; 35.4; 35.3; 31.7; 31.6; 31.3. HR-ESI-MS: 973.5888 ($[M + H]^{+}$, $C_{72}H_{77}O_2^{+}$; calc. 973.5918). Crystal suitable for X-ray diffraction was obtained by slow evaporation of solvent from a $CD_2Cl_2$ solution (see *Supporting Information*, *Section S6*).

## Supplementary Material

Supporting information for this article is available on the WWW under https://doi.org/10.1002/hlca.201900004. A summary of crystallographic data is available as ESI, and the structures deposited with the Cambridge Structural Database (CCDC deposition numbers: 1885359 for (±)-**3$^{b}$**, 1883711 for *meso*-**3$^{c}$**, 1883712 for (±)-**3$^{c}$**, and 1885360 for (±)-**3$^{d}$**). These data can be obtained free of charge from *The Cambridge Crystallographic Data Centre via* www.ccdc.cam.ac.uk/data_request/cif.

## Acknowledgements

*D. B.* gratefully acknowledges the EU through the MSCA-RISE project 'INFUSION' (Project ID: 734834) and Cardiff University. *T. M.*, *D. B.*, and *G. B.* thank the MIUR-FIRB Futuro in Ricerca SUPRACARBON (Project ID: RBFR10DAK6) and University of Trieste. *G. B.* acknowledges the CINECA award under the ISCRA initiative for the HPC resources and support. We thank Dr. *Robert L. Jenkins* for the help with 600 MHz- and VT-NMR experiments, *Thomas Williams* for his support with HR-MALDI-MS analysis, and the Analytical Service at the School of Chemistry, Cardiff University.

## Author Contribution Statement

*T. M.* performed all the syntheses and the photo-physical characterization. *T. M.* and *D. B.* wrote the manuscript through contribution of all authors. *N. B.* and *B. M. K.* solved and refined the X-Ray diffraction structures of compounds *meso*-**3**$^{c}$ and (**?**)-**3**$^{c}$, while *N. D.* performed the X-ray diffraction structural charac-terizations of molecules (**?**)-**3**$^{b}$ and (**?**)-**3**$^{d}$. *N. B.* and *G. B.* performed the computational studies. *T. M.* and *D. B.* programmed and coordinated all the scientific activities.

## References


[1] T. K. Ahn, K. S. Kim, D. Y. Kim, S. B. Noh, N. Aratani, C. Ikeda, A. Osuka, D. Kim, 'Relationship between Two-Photon Absorption and the π-Conjugation Pathway in Porphyrin Arrays through Dihedral Angle Control', *J. Am. Chem. Soc.* **2006**, *128*, 1700–1704.

[2] N. Yoshida, T. Ishizuka, A. Osuka, D. H. Jeong, H. S. Cho, D. Kim, Y. Matsuzaki, A. Nogami, K. Tanaka, 'Fine Tuning of Photophysical Properties of *meso meso*-Linked $Zn^{II}$ Diporphyrins by Dihedral Angle Control', *Chem. Eur. J.* **2003**, *9*, 58 –75.

[3] K. Takaishi, M. Kawamoto, K. Tsubaki, 'Multibridged Chiral Naphthalene Oligomers with Continuous Extreme-Cisoid Conformation', *Org. Lett.* **2010**, *12*, 1832–1835.

[4] K. Nakanishi, D. Fukatsu, K. Takaishi, T. Tsuji, K. Uenaka, K. Kuramochi, T. Kawabata, K. Tsubaki, 'Oligonaphthofurans: Fan-Shaped and Three-Dimensional π-Compounds', *J. Am. Chem. Soc.* **2014**, *136*, 7101 –7109.

[5] Z. Chen, U. Baumeister, C. Tschierske, F. Würthner, 'Effect of Core Twisting on Self-Assembly and Optical Properties of Perylene Bisimide Dyes in Solution and Columnar Liquid Crystalline Phases', *Chem. Eur. J.* **2007**, *13*, 450– 465.

[6] J. Roncali, 'Molecular Engineering of the Band Gap of π-Conjugated Systems: Facing Technological Applications', *Macromol. Rapid Commun.* **2007**, *28*, 1761 –1775.

[7] T. Miletić, A. Fermi, I. Orfanos, A. Avramopoulos, F. De Leo, N. Demitri, G. Bergamini, P. Ceroni, M. G. Papadopoulos, S. Couris, D. Bonifazi, 'Tailoring Colors by O Annulation of Polycyclic Aromatic Hydrocarbons', *Chem. Eur. J.* **2017**, *23*, 2363 –2378.

[8] M. J. Guberman-Pfeffer, J. A. Greco, L. P. Samankumara, M. Zeller, R. R. Birge, J. A. Gascón, C. Brückner, 'Bacteriochlor-ins with a Twist: Discovery of a Unique Mechanism to Red-Shift the Optical Spectra of Bacteriochlorins', *J. Am. Chem. Soc.* **2017**, *139*, 548–560.

[9] K. Nakanishi, T. Sasamori, K. Kuramochi, N. Tokitoh, T. Kawabata, K. Tsubaki, 'Synthesis and Properties of Butter-fly-Shaped Expanded Naphthofuran Derivatives', *J. Org. Chem.* **2014**, *79*, 2625– 2631.

[10] Y. Wang, Y. Li, S. Liu, F. Li, C. Zhu, S. Li, Y. Cheng, 'Regulating Circularly Polarized Luminescence Signals of Chiral Binaphthyl-Based Conjugated Polymers by Tuning Dihedral Angles of Binaphthyl Moieties', *Macromolecules* **2016**, *49*, 5444 –5451.

[11] J. M. Brunel, 'Update 1 of: BINOL: A Versatile Chiral Reagent', *Chem. Rev.* **2007**, *107*, PR1–PR45.

[12] S. Gladiali, E. Alberico, K. Junge, M. Beller, '*BINEPINES*: Chiral Binaphthalene-Core Monophosphepine Ligands for Multi-purpose Asymmetric Catalysis', *Chem. Soc. Rev.* **2011**, *40*, 3744 –3763.

[13] M. M. Pereira, M. J. F. Calvete, R. M. B. Carrilho, A. R. Abreu, 'Synthesis of binaphthyl based phosphine and phosphite ligands', *Chem. Soc. Rev.* **2013**, *42*, 6990– 7027.

[14] K. Tanaka, 'Catalytic Enantioselective Synthesis of Planar Chiral Cyclophanes', *Bull. Chem. Soc. Jpn.* **2018**, *91*, 187 – 194.

[15] O. Baudoin, D. Guénard, F. Guéritte, 'Palladium-Catalyzed Borylation of Ortho-Substituted Phenyl Halides and Application to the One-Pot Synthesis of 2,2'-Disubstituted Biphenyls', *J. Org. Chem.* **2000**, *65*, 9268 –9271.

[16] G. Bringmann, T. Gulder, T. A. M. Gulder, M. Breuning, 'Atroposelective Total Synthesis of Axially Chiral Biaryl Natural Products', *Chem. Rev.* **2011**, *111*, 563–639.

[17] I. Cepanec, 'Synthesis of Biaryls', Elsevier Science Ltd., Oxford, 2004.

[18] P. Devendar, R.-Y. Qu, W.-M. Kang, B. He, G.-F. Yang, 'Palladium-Catalyzed Cross-Coupling Reactions: A Powerful Tool for the Synthesis of Agrochemicals', *J. Agric. Food Chem.* **2018**, *66*, 8914 –8934.

[19] J. Cuntze, L. Owens, V. Alcázar, P. Seiler, F. Diederich, 'Molecular Clefts Derived from 9,9'-spirobi[9*H*-fluorene] for enantioselective complexation of pyranosides and dicarboxylic acids', *Helv. Chim. Acta* **1995**, *78*, 367–390.

[20] B. B. Frank, B. Camafort Blanco, S. Jakob, F. Ferroni, S. Pieraccini, A. Ferrarini, C. Boudon, J.-P. Gisselbrecht, P. Seiler, G. P. Spada, F. Diederich, '*N*-Arylated 3,5-Dihydro-4*H*-dinaphtho[2,1-*c* : 1',2'-*e*]azepines: Axially Chiral Donors with High Helical Twisting Powers for Nonplanar Push Pull Chromophores', *Chem. Eur. J.* **2009**, *15*, 9005 –9016.

[21] L. Đorđević, T. Marangoni, T. Miletić, J. Rubio-Magnieto, J. Mohanraj, H. Amenitsch, D. Pasini, N. Liaros, S. Couris, N. Armaroli, M. Surin, D. Bonifazi, 'Solvent Molding of Organic Morphologies Made of Supramolecular Chiral Polymers', *J. Am. Chem. Soc.* **2015**, *137*, 8150 –8160.

[22] N. Noujeim, L. Leclerq, A. R. Schmitzer, 'Imidazolium Cations in Organic Chemistry: From Chemzymes to Supramolecular Building Blocs', *Curr. Org. Chem.* **2010**, *14*, 1500 –1516.

[23] Y.-L. Wu, F. Ferroni, S. Pieraccini, W. B. Schweizer, B. B. Frank, G. P. Spada, F. Diederich, '1,2-Di(phenylethynyl) ethenes with axially chiral, 2,2'-bridged 1,1'-binaphthyl substituents: potent cholesteric liquid-crystal inducers', *Org. Biomol. Chem.* **2012**, *10*, 8016 –8026.

[24] O. Gidron, M.-O. Ebert, N. Trapp, F. Diederich, 'Chiroptical Detection of Nonchromophoric, Achiral Guests by Enantio-pure Alleno-Acetylenic Helicages', *Angew. Chem. Int. Ed.* **2014**, *53*, 13614 –13618.

[25] N. Sakai, K. C. Brennan, L. A. Weiss, S. Matile, 'Toward Biomimetic Ion Channels Formed by Rigid-Rod Molecules: Length-Dependent Ion-Transport Activity of Substituted Oligo(*p*-Phenylene)s', *J. Am. Chem. Soc.* **1997**, *119*, 8726 – 8727.

[26] K. W. Bentley, L. A. Joyce, E. C. Sherer, H. Sheng, C. Wolf, C. J. Welch, 'Antenna Biphenols: Development of Extended Wavelength Chiroptical Reporters', *J. Org. Chem.* **2016**, *81*, 1185 –1191.

[27] S. A. McFarland, N. S. Finney, 'Fluorescent Chemosensors Based on Conformational Restriction of a Biaryl Fluorophore', *J. Am. Chem. Soc.* **2001**, *123*, 1260 –1261.

[28] Q. Verolet, A. Rosspeintner, S. Soleimanpour, N. Sakai, E. Vauthey, S. Matile, 'Turn-On Sulfide $\pi$ Donors: An Ultrafast Push for Twisted Mechanophores', *J. Am. Chem. Soc.* **2015**, *137*, 15644 –15647.

[29] L. Maggini, D. Bonifazi, 'Hierarchised luminescent organic architectures: design, synthesis, self-assembly, self-organisation and functions', *Chem. Soc. Rev.* **2012**, *41*, 211 –241.

[30] L.-Z. Gong, Q.-S. Hu, L. Pu, 'Optically Active Dendrimers with a Binaphthyl Core and Phenylene Dendrons: Light Harvesting and Enantioselective Fluorescent Sensing', *J. Org. Chem.* **2001**, *66*, 2358 –2367.

[31] G. Wei, Y. Jiang, F. Li, Y. Quan, Y. Cheng, C. Zhu, ''Click'-BINOL based chiral ionic polymers for highly enantioselec-tive recognition of tryptophan anions', *Polym. Chem.* **2014**, *5*, 5218 –5222.

[32] L. Pu, 'Enantioselective Fluorescent Sensors: A Tale of BINOL', *Acc. Chem. Res.* **2012**, *45*, 150–163.

[33] X. Zhang, J. Yin, J. Yoon, 'Recent Advances in Development of Chiral Fluorescent and Colorimetric Sensors', *Chem. Rev.* **2014**, *114*, 4918–4959.

[34] K. Ariga, H. Ito, J. P. Hill, H. Tsukube, 'Molecular Recog-nition: from Solution Science to Nano/Materials Technol-ogy', *Chem. Soc. Rev.* **2012**, *41*, 5800 –5835.

[35] D. Ishikawa, T. Mori, Y. Yonamine, W. Nakanishi, D. L. Cheung, J. P. Hill, K. Ariga, 'Mechanochemical Tuning of the Binaphthyl Conformation at the Air Water Interface', *Angew. Chem. Int. Ed.* **2015**, *127*, 9116– 9119.

[36] K. Ariga, G. J. Richards, S. Ishihara, H. Izawa, J. P. Hill, 'Intelligent Chiral Sensing Based on Supramolecular and Interfacial Concepts', *Sensors* **2010**, *10*, 6796 –6820.

[37] R. Pinalli, A. Pedrini, E. Dalcanale, 'Environmental Gas Sensing with Cavitands', *Chem. Eur. J.* **2018**, *24*, 1010 – 1019.

[38] W. P. Lustig, S. Mukherjee, N. D. Rudd, A. V. Desai, J. Li, S. K. Ghosh, 'Metal organic frameworks: functional luminescent and photonic materials for sensing applications', *Chem. Soc. Rev.* **2017**, *46*, 3242 –3285.

[39] F. Meng, F. Li, L. Yang, Y. Wang, Y. Quan, Y. Cheng, 'The Amplified Circularly Polarized Luminescence Emission Response of Chiral 1,1'-Binaphthol-Based Polymers via Zn(II)-Coordination Fluorescence Enhancement', *J. Polym. Sci., Part A: Polym. Chem.* **2018**, *56*, 1282 –1288.

[40] T. Shimasaki, S. Kato, K. Ideta, K. Goto, T. Shinmyozu, 'Synthesis and Structural and Photoswitchable Properties of Novel Chiral Host Molecules: Axis Chiral 2,2'-Dihydroxy-1,1'-binaphthyl-Appended *stiff*-Stilbene', *J. Org. Chem.* **2007**, *72*, 1073 –1087.

[41] J. Wang, B. L. Feringa, 'Dynamic Control of Chiral Space in a Catalytic Asymmetric Reaction Using a Molecular Motor', *Science* **2011**, *331*, 1429– 1432.

[42] S. F. Pizzolato, P. Štacko, J. C. M. Kistemaker, T. van Leeuwen, E. Otten, B. L. Feringa, 'Central-to-Helical-to-Axial-to-Central Transfer of Chirality with a Photoresponsive Catalyst', *J. Am. Chem. Soc.* **2018**, *140*, 17278–17289.

[43] W.-H. Soe, Y. Shirai, C. Durand, Y. Yonamine, K. Minami, X. Bouju, M. Kolmer, K. Ariga, C. Joachim, W. Nakanishi, 'Conformation Manipulation and Motion of a Double Paddle Molecule on an Au(111) Surface', *ACS Nano* **2017**, *11*, 10357 – 10365.

[44] J. J. G. S. van Es, H. A. M. Biemans, E. W. Meijer, 'Synthesis and characterization of optically active cyclic 6,6'-dinitro-1,1'-binaphthyl-2,2'-diethers', *Tetrahedron: Asymmetry* **1997**, *8*, 1825 –1831.

[45] Q. Sun, Z. Dai, X. Meng, F.-S. Xiao, 'Homochiral Porous Framework as a Platform for Durability Enhancement of Molecular Catalysts', *Chem. Mater.* **2017**, *29*, 5720 –5726.

[46] J. E. Simpson, G. H. Daub, F. N. Hayes, 'Synthesis of Some 2,2'-Dioxa-Bridged Biphenyls and 1,1'-Binaphthyls', *J. Org. Chem.* **1973**, *38*, 1771 –1771.

[47] D. Mosca, A. Stopin, J. Wouters, N. Demitri, D. Bonifazi, 'Stereospecific Winding of Polycyclic Aromatic Hydrocar-bons into Trinacria Propellers', *Chem. Eur. J.* **2017**, *23*, 15348 –15354.

[48] M. J. Frisch, G. W. Trucks, H. B. Schlegel, G. E. Scuseria, M. A. Robb, J. R. Cheeseman, G. Scalmani, V. Barone, B. Mennuc-ci, G. A. Petersson, H. Nakatsuji, M. Caricato, X. Li, H. P. Hratchian, A. F. Izmaylov, J. Bloino, G. Zheng, J. L. Sonnenberg, M. Hada, M. Ehara, K. Toyota, R. Fukuda, J. Hasegawa, M. Ishida, T. Nakajima, Y. Honda, O. Kitao, H. Nakai, T. Vreven, J. A. Montgomery Jr., J. E. Peralta, F. Ogliaro, M. Bearpark, J. J. Heyd, E. Brothers, K. N. Kudin, V. N. Staroverov, R. Kobayashi, J. Normand, K. Raghavachari, A. Rendell, J. C. Burant, S. S. Iyengar, J. Tomasi, M. Cossi, N. Rega, J. M. Millam, M. Klene, J. E. Knox, J. B. Cross, V. Bakken, C.Adamo, J. Jaramillo, R. Gomperts, R. E. Stratmann, O. Yazyev, A. J. Austin, R. Cammi, C. Pomelli, J. W. Ochterski, R. L. Martin, K. Morokuma, V. G. Zakrzewski, G. A. Voth, P. Salvador, J. J. Dannenberg, S. Dapprich, A. D. Daniels, Ö. Farkas, J. B. Foresman, J. V. Ortiz, J. Cioslowski, D. J. Fox, Gaussian 09, Revision D.01, Gaussian, Inc., Wallingford CT, 2009.